Biosynthesis and apical localization of the urokinase receptor in polarized MDCK epithelial cells

Paola Limongi[a], Massimo Resnati[a], Luciano Hernandez-Marrero[a], Ottavio Cremona[b], Francesco Blasi[a], Francesca Fazioli[a,*]

[a]*Department of Biological and Technological Research (DIBIT), San Raffaele Scientific Institute, and Department of Genetics and Microbial Biology, University of Milan, Via Olgettina 60, 20132 Milan, Italy*

[b]*Dipartimento di Scienze Mediche, University of Torino, Branch of Novara, Via Solaroli 17, Novara, Italy*

Received 12 June 1995

Abstract The biosynthesis and the surface localization of the urokinase plasminogen activator receptor (uPAR) were analysed in MDCK epithelial cells and in unpolarized fibroblasts. No differences were observed with respect to rate of synthesis, nature of precursors and time of surface appearance. uPAR was localized particularly at the focal and cell-cell contacts when expressed in fibroblasts. On the contrary, in MDCK cells uPAR was found mostly on the apical surface; in agreement with its localization, down-regulation of uPAR by the uPA–PAI-1 complex was observed only from the apical membrane.

Key words: Urokinase receptor; GPI-anchored protein; MDCK cell

1. Introduction

The urokinase-type plasminogen activator (uPA) and its receptor (uPAR) are at the center of a complex network affecting cell movement and thus are involved in many different physiological processes as well as pathological conditions [1,2]. uPAR is a heavily glycosylated protein with a molecular weight of 55,000–60,000, composed of three internal homologous domains and anchored to the plasma membrane by a glycosylphosphatidylinositol (GPI) linkage [1,2]. The receptor for uPA is central to the pleiotropic functions of uPA, modulating pro-uPA activation, focusing uPA activity to the cell surface and favoring the internalization of uPA/inhibitors complexes [3]. In addition, receptor binding can modulate cell adhesion, migration or growth through direct mechanisms of signal transduction [4–6].

Immunofluorescence and electron microscopy studies have identified uPA and uPAR at discrete cell–cell and cell–substratum contact sites [7–9], in agreement with a function in the degradation of extra-cellular matrix and thus in cell migration. However, this localization contradicts the notion that GPI anchored proteins are sorted preferentially to the apical surface in polarized epithelial cells [10,11]. Here, we have analyzed the biosynthesis of uPAR and its surface expression, studying the time of appearance, the nature of precursors and the localization in polarized epithelial cells and in unpolarized fibroblasts.

*Corresponding author. Fax: (39) (2) 2643 4844.

Abbreviations: uPA, urokinase-type plasminogen activator; pro-uPA, pro-urokinase; uPAR, urokinase-type plasminogen activator receptor; GPI, glycosylphosphatidylinositol; ATF, amino-terminal fragment of uPA; PAI-1, plasminogen activator inhibitor type-1; PI-PLC, phosphatidylinositol-specific phospholipase C; Sulfo-NHS-Biotin, sulfosuccinimidobiotin; DSS, *N,N'*-disuccinimidyl suberate; TX-100, Triton X-100; MDCK, Madin–Darby canine kidney cells.

2. Materials and methods

2.1. Materials

Following reagents were kindly donated: monoclonal anti-uPAR antibodies R2, R3, R4 [12] by E. Rønne and G. Høyer-Hansen and were purified by G-Protein affinity cromatography (Mab-Trap, Pharmacia); monoclonal antibody recognizing the Na^+/K^+-ATPase alfa subunit [13] by M.J. Caplan; ATF, the amino-terminal fragment of uPA (residues 1–143) by J. Henkin; two chain uPA by M.L. Nolli; recombinant active PAI-1 [14] by D. Ginsburg. Rabbit anti-uPAR polyclonal serum was obtained by immunizing animals with a purified soluble form of uPAR (suPAR) [15] and was affinity purified on a suPAR-conjugated agarose column. Rhodamine-conjugated swine anti-rabbit IgG were from Dakopatts. PI-PLC from *B. cereus* and endoglycosidase H were from Boehringer Mannheim GmbH. Sulfosuccinimidobiotin (Sulfo-NHS-Biotin) and *N,N'*-disuccinimidyl suberate (DSS) were from Pierce. Phenylmethylsulfonyl fluoride (PMSF), *n*-Butyric acid sodium salt, tunicamicyn, strepdavidin-agarose and mouse IgG_1 (MOPC-21) were from Sigma. The uPA–PAI-1 complexes were formed as previously described [16].

2.2. Cell culture and transfections

Cells were grown continuously as monolayers in Dulbecco's Modified Eagle's medium (D-MEM) supplemented with 5% fetal calf serum. LB6 Clone 19 cells have been previously described [17]. MDCK cells (strain II) [18] were a kind gift from Dr. K. Simons (E.M.B.L., Heidelberg, Germany). Polarization of MDCK cells was ensured by growing monolayers for at least 6 days on Transwell filters.

DNA transfection was performed by the calcium phosphate precipitation technique [19].

2.3. Cross-linking, binding assay and immunofluorescence

Iodination of ATF, cross-linking of [^{125}I]ATF to uPAR with DSS, Triton X-114 phase separation and PI-PLC treatment were carried out as described [20]. Binding assays on cells plated for 24 hours on a 96-well plate, was carried out with iodinated ATF, as described [17].

Polarized monolayers of MDCK/uPAR were fixed in 3% paraformaldehyde in pH 7.4 PBS-sucrose (2%) for 15 min at room temperature, rinsed, and incubated 1 h at 37°C with polyclonal anti-uPAR antibodies (20 μg/ml). Antibodies were added from both the apical and the basolateral compartements. Visualization and microscopy followed standard procedures. Samples were analysed with a Sarastro 2000 confocal laser scanning microscope (Molecular Dynamics) fitted onto an Axiophot fluorescence microscope (Zeiss). Data are presented both as serial optical sections of 0.2 μm in the *Z* axis or as projections in the *X, Y* plane.

2.4. Metabolic labeling and immunoprecipitation

Confluent cells monolayers were stimulated overnight with 10 mM sodium butyrate in D-MEM + 5% FCS; cells were subsequently starved for 30 min in methionine- and cysteine-free D-MEM and pulse-labeled at 37°C with 300 μCi/ml of [^{35}S]-*Trans*Label (ICN). Cells were thus chased in complete medium (D-MEM + 5% FCS + 10 mM methionine

SSDI 0014-5793(95)00742-3

and cysteine) for the indicated times. Extracts were made in StaphA buffer (10 mM sodium phosphate, pH 7.4, 150 mM NaCl, 1% TX-100, 0.5% deoxycholate, 0.1% SDS, 2 mM PMSF and 50 μg/ml aprotinin). When appropriate, tunicamycin (2 μg/ml) was added to the medium for 1 h before the addition of radioactive label and included during the pulse and chase periods.

Lysates were precleared with an irrelevant isotype-matched mAb (MOPC-21) coupled to GammaBind-G Sepharose (Pharmacia) and the supernatants immunoprecipitated with the indicated antibodies with GammaBind-G Sepharose. For digestion with Endoglycosidase H, immuno complexes were treated overnight at 4°C with 50 mU/ml endoglycosidase H in 20 mM sodium phosphate, pH 6.0, 20 mM NaCl.

2.5. Domain-selective cell surface biotinylation

Surface localization of uPAR on polarized MDCK cells was tested by treating cells with sulfo-NHS-Biotin (1 mg/ml) added to the basolateral (1,5 ml) or to the apical compartment (0.5 ml) of the Transwell unit. Cells were handled as described [21], extracted in StaphA buffer, immunoprecipitated, electrophoresed and transferred on nitrocellulose. Biotinylated proteins were detected with [^{125}I]streptavidin (Amersham). In some experiments, before selective cell surface biotinylation, cells were first incubated with ligands, applied to either the apical or the basolateral surface of cell monolayers, at 4°C for two hours.

3. Results

3.1. Characterization of MDCK, NIH3T3 and LB6 cells expressing transfected human uPAR

An SV40-driven full length human uPAR cDNA [17] was transfected into NIH-3T3 or MDCK strain II cells. Stably transfected LB6 cells expressing human uPAR have already been described [17]. Proper expression of uPAR was assessed by immunoblotting, sensitivity to PI-PLC, phase separation in Triton X-114, electrophoretic mobility and direct binding experiments. These experiments showed that all clones expressed a ca. 55 kDa human uPAR properly GPI-anchored in the membrane, as demonstrated by PI-PLC sensitivity (not shown). Clones were chosen (henceforth referred to as NIH/uPAR, MDCK/uPAR and LB6 Clone 19) displaying a comparable number of receptors (approximately 6–8 × 10^5 binding sites per cell). Scatchard plot analysis indicated a single class of binding sites with similar affinity towards [^{125}I]ATF (data not shown).

3.2. Immunolocalization of uPAR on the cell surface

In polarized epithelial cells GPI-anchored proteins are preferentially targeted to the apical surface [10,11]. We analyzed the distribution of uPAR in non permeabilized polarized MDCK cells, by indirect immunofluorescence and laser scanning confocal microscopy. In parallel, analysis of the cell surface distribution of uPAR was also performed on non permealized NIH/uPAR and LB6 Clone 19 cells. Controls using pre-immune sera or secondary antibodies alone gave no staining (data not shown). Fig. 1 shows serial optical sections from the basal to the apical membrane of MDCK/uPAR. Strong staining was detected at the apical surface (i.e. sections in panels g to j), indicating that the receptor was particularly concentrated at this pole of the cells; in addition, uPAR was also localized along the lateral surface, as shown by the strong inter-cellular staining. The signal of MDCK/uPAR cells showed a punctate pattern,

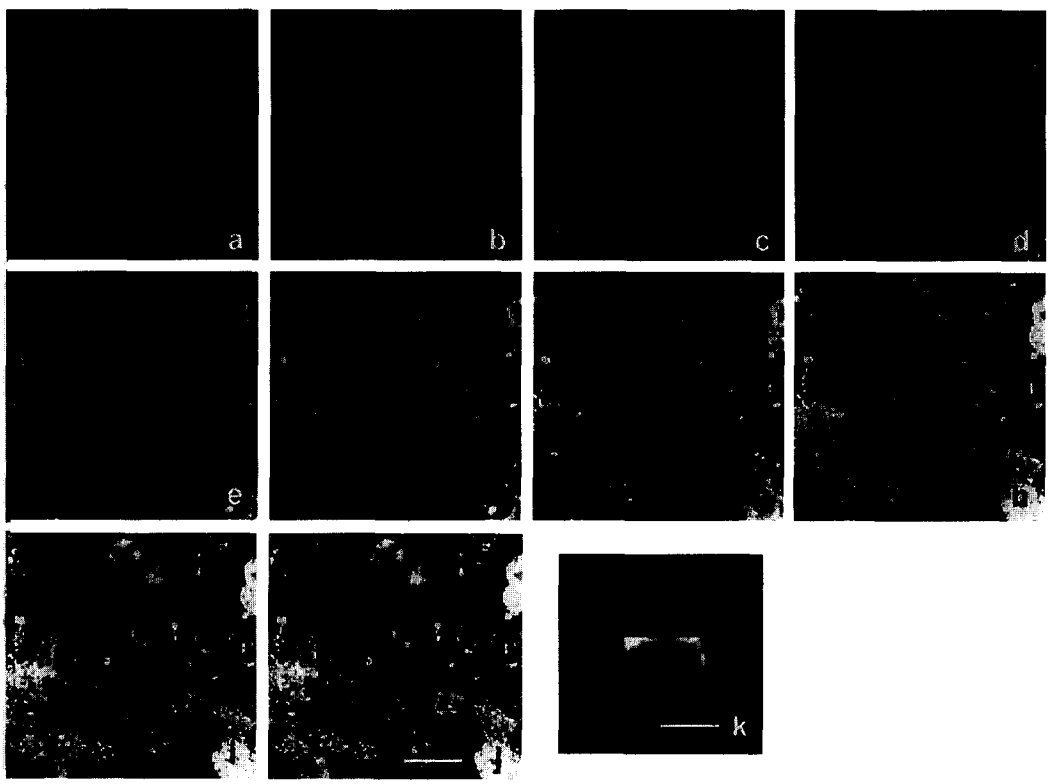

Fig. 1. Immuno-localization of uPAR on non permealized polarized MDCK/uPAR cells. MDCK/uPAR cells were grown on Transwell filters, fixed with 3% paraformaldehyde, incubated with an affinity purified rabbit anti-uPAR polyclonal antibody (20 μg/ml) added to both the apical and the basolateral compartments and revealed with a rhodamine-conjugated swine anti-rabbit IgG (30 μg/ml). Optical sections increasing by 0.5 mm along the *Z* axis, obtained with a scanning laser confocal microscope, are shown from the basal (a) to the apical level (j). A sagittal projection of one cell is also shown (k). Bars = (a–j) 24 mm, (k) 7 mm.

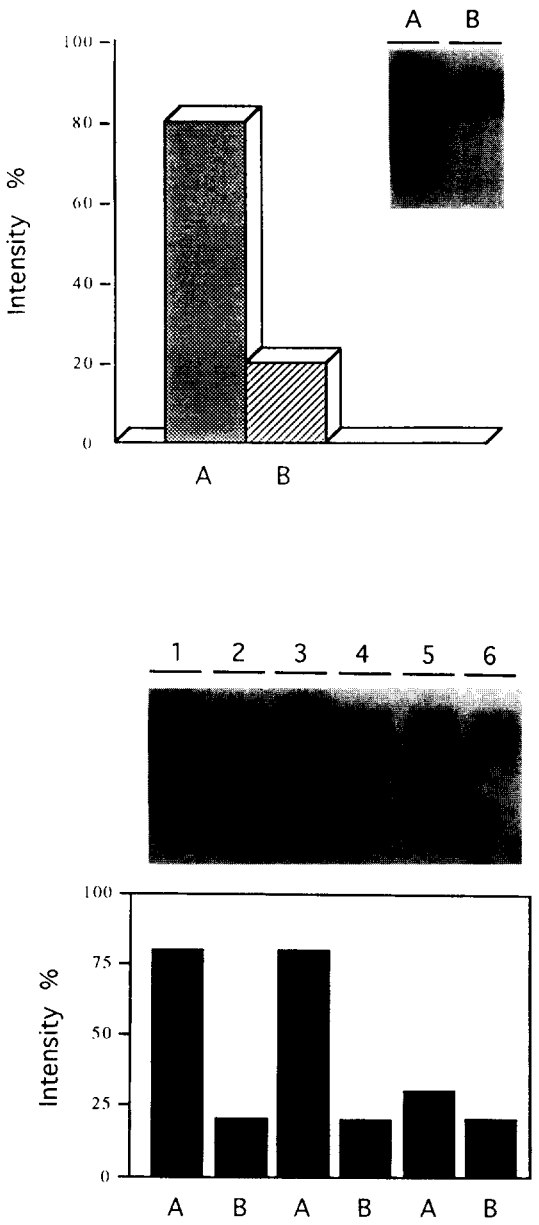

Fig. 2. Surface expression and uPA/PAI-1-induced downregulation of uPAR in polarized MDCK/uPAR cells. Top: Polarized MDCK/uPAR cells, grown on Transwell filters, were biotinylated either on the apical (A) or the basolateral surface (B). Cell extracts were immunoprecipitated with anti-uPAR mAbs, run on SDS-PAGE, transferred to nitrocellulose and probed with [^{125}I]strepdavidin (Inset). Autoradiograms from three independent experiments were quantitated by densitometric scans and results expressed as percent of apical (A) or basolateral (B) uPAR surface expression. Bottom: Filter grown MDCK/uPAR cells were incubated with binding medium alone (lanes 1 and 2), 10 nM free uPA (lanes 3 and 4) or 10 nM preformed uPA–PAI-1 complexes (lanes 5 and 6) for 2 h at 4°C. Ligands were added either to the apical (A) or the basolateral (B) compartment of the Transwell unit. Cells were shifted at 37°C for 1 h to allow internalization of uPAR, biotinylated, lysed and immunoprecipitated as in the top panel. Quantitative measurements were obtained by densitometric scanning of autoradiograms from two independent experiments and results expressed as percent of uPAR in the apical (A) or basolateral (B) compartment.

indicating a clustered distribution of uPAR at the cell surface. No basal membrane staining was observed (see sections in panels a, b). The data of the optical sections a through j were saved as 512 × 512 pixed images and then processed as TIFF files, on a Silicon Graphics Workstation to reconstruct a sagittal projection. The apical and lateral localization of uPAR was even clearer in this reconstructed projection (Fig. 1, panel k). In NIH/uPAR cells, a different distribution was observed, similar to that previously reported [9]: the receptor appeared in discrete patches of staining, localized primarily to cell-cell borders and to cell–substratum contact areas (ventral face), while it was almost completely absent at more apical levels (not shown). A similar staining pattern was obtained in LB6/uPAR cells (not shown).

Apical surface distribution of uPAR in polarized MDCK/uPAR cells was also investigated by domain selective surface biotinylation. Polarized MDCK/uPAR cells were selectively labeled either from the apical or the basolateral surface with sulfo-NHS-biotin, lysed, immunoprecipitated with specific anti-uPAR antibodies and revealed by blotting, binding to [^{125}I]streptavidin and autoradiography (Fig. 2A, inset). As a marker for basolateral localization, we used antibodies directed towards the alfa subunit of Na^+/K^+ ATPase [13]. Results of three independent experiments, summarized in Fig. 2A, showed that uPAR was preferentially expressed on the apical surface of MDCK cells (82% apical), while the Na^+/K^+ ATPase showed the typical basolateral localization (more than 98% basolateral) (not shown). The electrophoretic analysis of the immunoprecipitated biotynylated uPAR revealed, in addition to the 55 kDa band, a second 40–50 kDa band (Fig. 2A, inset), most probably representing the cleaved uPAR lacking the ligand-binding domain 1, described for other cell lines [22]. In fact, while the 40–55 kDa variant could be also observed in Western blot experiments using R2 antibodies, it did not show up in crosslinking assays (not shown). A similar result was observed in NIH/uPAR and LB6 Clone 19 cells under the same experimental conditions (not shown).

3.3. *Biosynthesis of uPAR in MDCK cells and fibroblasts*

We next carried out pulse-chase experiments to investigate the biogenesis of newly synthesized uPAR. LB6/uPAR cells were pulse-labeled with [^{35}S]-*Trans*Label for 15 min, chased for various times and solubilized with StaphA buffer (see section 2). Immunoprecipitates obtained with a mixture of three anti-uPAR monoclonal antibodies (R2, R3 and R4) [12] were analyzed by SDS-PAGE and fluorography. As a control, an irrelevant isotype-matched monoclonal antibody was used (Fig. 3A, first lane). After the pulse, two polypeptides of 41 and 44 kDa were specifically immunoprecipitated by the anti-uPAR mAbs (Fig. 3A). During the chase period, the label in these polypeptides decreased and the mature receptor (55–60 kDa) began to appear. By 2 hours, mature uPAR was the only labeled polypeptide immunoprecipitated. Similar data were obtained with a 5 min pulse, except that most of the radioactivity was incorporated into the 41 kDa polypeptide (not shown). The 41 and 44 kDa bands may represent immature glycosylation products. To test this point, digestion of the immunoprecipitates with endoglycosidase H was carried out. While this treatment did not alter the migration of the 55–60 kDa band in SDS-PAGE (as previously reported) [23], the apparent molecular weight of the precursor was reduced from the 41 and 44 kDa to 32 kDa (Fig. 3C). Further proof was obtained by pretreatment of the cells with tunicamycin, a drug that completely inhibits addition of all N-linked oligosaccharide chains [24]. Under these condi-

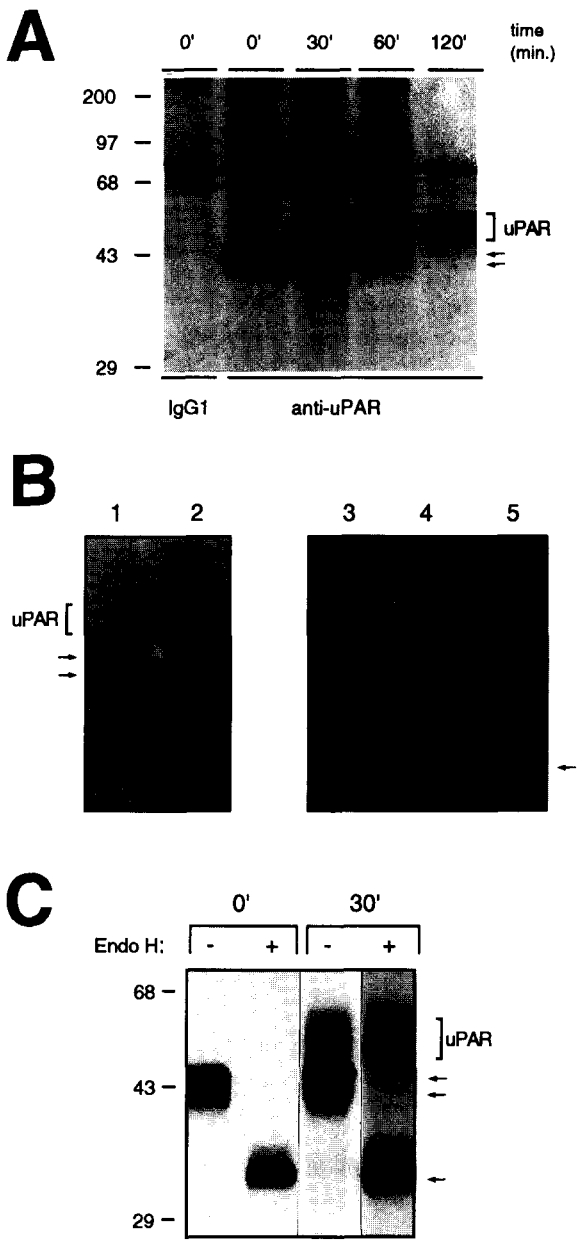

Fig. 3. Biosynthesis of uPAR in LB6 Clone 19. (A) LB6 clone 19 cells were pulse labeled with [^{35}S]*Trans*Label for 15 min and chased for the indicated times (see section 2). Cells were lysed, immunoprecipitated with anti-uPAR antibodies and analysed by SDS-PAGE. Control immunoprecipitation with an irrelevant isotype-matched antibody of lysates at 0 min chasing time is shown in the first lane. Arrows indicate the 41 and 44 kDa uPAR precursors. The position of the mature form of uPAR is also indicated. (B) Effect of tunicamycin on uPAR biosynthesis. LB6 Clone 19 cells were pre-incubated for 1 h at 37°C in labeling medium in absence (left panel) or in presence of 2 mg/ml tunicamycin (right panel). Cells were then pulse-labeled for 15 min and then directly lysed (lanes 1, 3 and 4) or chased for 2 h before lysis (lanes 2 and 5). Tunicamycin, when present, was maintained at the same concentration throughout the experiment. Lanes 1, 2, 4 and 5 represent immunoprecipitates with anti-uPAR mAbs, lane 3 represents an immunoprecipitation with an irrelevant IgG1 mAb. The position of the 32 kDa not-glycosylated uPAR is shown by an arrow on the right. (C) Effect of endoglycosidase H digestion on uPAR-precursors. LB6 clone 19 cells were pulse-labeled, chased for the indicated times, lysed and immunoprecipitated. Immuno complexes were recovered on GammaBind G Sepharose, resuspended, incubated with (+) or without (−) 50 mU/ml endoglycosidase H and electrophoresed. The position of the 41 and 44 kDa precursors and 32 kDa deglycosylated uPAR are indicated by an arrow on the right.
←

tions, again the 32 kDa band (arrow) appeared as the only specific immunoprecipitated product (Fig. 3B). When the same experiments were performed in NIH/uPAR and polarized MDCK/uPAR, we observed an identical pattern as well as identical timing for uPAR maturation (not shown). Thus, biosynthesis of uPAR seems to follow the same pattern in both polarized and unpolarized cells.

Surface appearance of mature uPAR was analysed by combining pulse-chase experiments with surface biotinylation [25]. Cells were pulse-labeled as described before and the appearance of surface uPAR was monitored by biotinylation at various periods of chase. To identify cell surface labeled uPAR, immunoprecipitates were boiled in 10% SDS buffer, reprecipitated with Streptavidin-agarose beads and analysed by fluorography, after SDS-PAGE. Mature uPAR appeared at the cell surface of NIH/uPAR, MDCK/uPAR and LB6 Clone 19 after 1 hour of chase (not shown) in agreement with the previous extimate.

3.4. *uPA–PAI-1 clearance from the cell surface of MDCK/uPAR*

Binding of uPA–PAI-1 complexes to uPAR results in the internalization and degradation of the ligand [26]. In human U937 cells, internalization of uPA–PAI-1 complexes is accompanied by down-regulation of uPAR [16]. This mechanism has been verified in several cell lines, including LB6 Clone 19 cells (not shown). Internalization and degradation of human uPA and uPA/PAI-1 pre-formed complexes were assayed in MDCK/uPAR cells. MDCK/uPAR cells were able to internalize and degrade human uPA/PAI-1 complexes, although with a lower efficiency than LB6 Clone 19 cells (data not shown). We therefore assayed for a differential downregulation of uPAR from the apical versus the basolateral surface of MDCK/uPAR cells. Polarized MDCK/uPAR cells, grown for several days on Transwell filters, were incubated at 4°C for two hours with uPA or with pre-formed uPA–PAI-1 complexes, added either to the apical or to the basolateral compartment of the Transwell unit. Cells were then shifted at 37°C for 1 h. After this time, whole cells were biotinylated, lysed and cell extracts immunoprecipitated with polyclonal anti-uPAR antibodies. As shown in Fig. 2B, the amount of mature uPAR immunoprecipitated from the apical surface of MDCK/uPAR incubated with uPA/PAI-1 complexes (Fig. 2B, lane 5), was clearly reduced with respect to cells incubated with free uPA (lane 3) or in the absence of ligand (lane 1). The down-regulation of uPAR did not affect the low molecular uPAR variant on the cell surface, as expected. On the other hand, no reduction was observed in the uPAR recovered from the basolateral compartment (Fig. 2B, lanes 2, 4, 6). We controlled that the efficiency of the anti-serum in immunoprecipitating free uPAR or uPAR/uPA and uPAR/uPA–PAI-1 complexes was indeed the same (not shown).

4. Discussion

We have analyzed the biosynthesis and cell surface localization of uPAR. The earliest precursor that could be visualized after a 5 min pulse was a 41–44 kDa doublet, whose molecular mass was decreased to a single band of 32 kDa upon endoglycosidase H treatment of the immunoprecipitated precursor, or tunicamycin treatment of the cells. Therefore the two 41 and 44 kDa bands represent differently glycosylated precursors. The minimum molecular weight, 32 kDa, is essentially identical to that of fully de-glycosylated mature uPAR [20] and to the size expected for the precursor on the basis of the amino acid sequence [17]. The nascent protein may have been already processed at the C-terminus and its GPI anchor attached. The migration of immunoprecipitated uPAR precursors did not change in different cell lines, nor did the time-course of maturation. In both fibroblastic LB6 and NIH-3T3 and in epithelial MDCK cells, human uPAR reached its full and final molecular weight in about one hour. At this time, biotinylation experiments in MDCK/uPAR cells showed that uPAR was beginning to appear on the apical cell surface.

In MDCK cells, uPAR was polarized at the apical and lateral surface as shown by immunofluorescence, domain-selective surface biotinylation and uPA/PAI-1-induced down-regulation. The polarized apical distribution of uPAR in MDCK cells compared to the nonpolarized, basal distribution in fibroblasts, suggests a differential function associated with the presence of uPAR at different sites. Apically, uPAR will have access to circulating uPA or uPA–PAI-1 complexes, and this may suggest a role in their clearance. The specific apical uPA–PAI-1 mediated down-modulation of uPAR is in line with this possibility. The fact that the addition of uPA–PAI-1 from the basolateral compartment did not lead to a down-regulation of uPAR, is in agreement with the presence of uPAR at sites not accessible to the medium. Whether the basal or apical distributions of uPAR reflect different functions awaits direct experimental proof.

Acknowledgements: We thank Drs. J. Henkin, Ebbe Rønne, G. Høyer-Hansen, M.L. Nolli, D. Ginsburg, K. Simons and M.J. Caplan for the generous gift of reagents. We are grateful to our colleagues Massimo Conese and L. Scotto for support and stimulating discussion. This work was supported by grants from the Associazione Italiana per la Ricerca sul Cancro (A.I.R.C.), Consiglio Nazionale delle Ricerche (P.F. A.C.R.O.) and Human Capital and Mobility Program of the E.C. (contract ERBCHRXCT 940427). P. Limongi is the recipient of a fellowship from H.S. Raffaele (Milan, Italy); L. Hernandez-Marrero is a recipient of a U.N.I.D.O. fellowship.

References

[1] Blasi, F., Conese, M., Møller, L.B., Pedersen, N., Cavallaro, U., Cubellis, M.V., Fazioli, F., Hernandez-Marrero, L., Limongi, P., Muñoz-Canoves, P., Resnati, M., Riitinen, L., Sidenius, N., Soravia, E., Soria, M.R., Stoppelli, M.P., Talarico,D., Teesalu, T. and Valcamonica, S. (1994) Fibrinolysis 8, Suppl. 1, 182–188.
[2] Danø, K., Behrendt, N., Brunner, N., Ellis, V., Ploug, M. and Pyke, C. (1994) Fibrinolysis 8, Suppl. 1, 189–203.
[3] Fazioli, F. and Blasi, F. (1994) Trends Pharm. Sci. 15, 25–29.
[4] Nusrat, A.R. and Chapman, A. Jr. (1991) J. Clin. Invest. 87, 1091–1097.
[5] Busso, N., Masur, S.K., Lazega, D., Waxman, S. and Ossowski, L. (1994) J. Cell. Biol. 126, 259–270.
[6] Rabbani, S.A., Mazar, A.P., Bernier, S.M., Haq, M., Bolivar, I., Henkin, J. and Goltzman, D. (1992) J. Biol. Chem. 267, 14151–14156.
[7] Pöllänen, J., Heldman, K., Nielsen, L.S., Danø, K. and Vaheri, A. (1988) J. Cell. Biol. 106, 87–95.
[8] Hébert, C.A. and Baker, J.B. (1988) J. Cell. Biol. 106, 1241–1247.
[9] Myöhäinen, H., Stephens, R.W., Hedman, K., Topiovaara, H., Rønne, E., Høyer-Hansen, G., Danø, K. and Vaheri, A. (1993) J. Hist. Cytochem. 41, 1291–1301.
[10] Lisanti, M.P., Caras, I.W., Davitz, M.A. and Rodriguez-Boulan, E. (1989) J. Cell. Biol. 109, 2145–2156.
[11] Brown, D.A., Crise, B. and Rose, J.K. (1989) Science 245, 1499–1501.
[12] Rønne, E., Behrendt, N., Ellis, V., Ploug, M., Danø, K. and Høyer-Hansen, G. (1991) FEBS Lett. 288, 233–236.
[13] Pietrini, G., Matteoli, M., Banker, G. and Caplan, M.J. (1992) Proc. Natl. Acad. Sci. USA 89, 8414–8418.
[14] Sherman, P.M., Lawrence, D.A., Yang, A.Y., Vanderberg, E.T., Paielli, D., Olson, S.T., Shore, J.D. and Ginsburg, D. (1992) J. Biol. Chem. 267, 7588–7595.
[15] Masucci, M.T., Pedersen, N. and Blasi, F. (1991) J. Biol. Chem. 266, 8655–8658.
[16] Olson, D., Pöllänen, J., Høyer-Hansen, G., Rønne, E., Sakaguchi, K., Wun, T.-C., Appella, E., Danø, K. and Blasi, F. (1992) J. Biol. Chem. 267, 9129–9133.
[17] Roldan, A.L., Cubellis, M.V., Masucci, M.T., Behrendt, N., Lund, L.R., Danø, K. and Blasi, F. (1990) EMBO J. 9, 467–474.
[18] Richardson, J.C.W., Scalera, V. and Simmons, N.L. (1981) Biochim. Biophys. Acta, 673, 26–36.
[19] Wigler, M., Pellicer, A., Silverstein, S., Axel, R., Urlaub, G. and Chasin, L. (1979) Proc. Natl. Acad. Sci. USA 76, 1373–1376.
[20] Behrendt, N., Rønne, E., Ploug, M., Petri, T., Lober, D., Nielsen, L.S., Schleuning, W.-D., Blasi, F., Appella, E. and Danø, K. (1990) J. Biol. Chem. 265, 6453–6460.
[21] Lisanti, M.P., Sargiacomo, M., Graeve, L., Saltiel, A.R. and Rodriguez-Boulan, E. (1988) Proc. Natl. Acad. Sci. USA 85, 9557–9561.
[22] Høyer-Hansen, G., Rønne, E., Solberg, H., Behrendt, N., Ploug, M., Lund, L.R., Ellis, V. and Danø, K. (1992) J. Biol. Chem. 267, 18244–18229.
[23] Møller, L.B., Pöllänen, J., Rønne, E., Pedersen, N. and Blasi, F. (1993) J. Biol. Chem. 268, 11152–11159.
[24] Struck, D.K. and Lennarz, W.J. (1977) J. Biol. Chem. 252, 1007–1013.
[25] Le Bivic, A., Real, F. and Rodriguez-Boulan, E. (1989) Proc. Natl. Acad. Sci. USA 86, 9313–9317.
[26] Cubellis, M.V., Wun, T.-C. and Blasi, F. (1990) EMBO J. 9, 1079–1085.